Radiation damage in silicon exposed to high-energy protons

Gordon Davies*
Department of Physics, King's College London, Strand, London WC2R 2LS, United Kingdom

Shusaku Hayama
Department of Physics, King's College London, Strand, London WC2R 2LS, United Kingdom
and CCLRC Daresbury Laboratory, Daresbury, Warrington, Cheshire, WA4 4AD, United Kingdom

Leonid Murin
Joint Institute of Solid State and Semiconductor Physics, National Academy of Sciences of Belarus, 220072 Minsk, Belarus

Reinhard Krause-Rehberg and Vladimir Bondarenko
Department of Physics, Martin Luther University, 06108 Halle, Germany

Asmita Sengupta
Department of Physics, Visva-Bharati Central University, Santiniketan-731235, India

Cinzia Davia and Anna Karpenko
Department of Electronic Engineering, Brunel University, Uxbridge UB8 3PH, United Kingdom
(Received 31 January 2006; published 3 April 2006)

Photoluminescence, infrared absorption, positron annihilation, and deep-level transient spectroscopy (DLTS) have been used to investigate the radiation damage produced by 24 GeV/c protons in crystalline silicon. The irradiation doses and the concentrations of carbon and oxygen in the samples have been chosen to monitor the mobility of the damage products. Single vacancies (and self-interstitials) are introduced at the rate of ~ 1 cm^{-1}, and divacancies at 0.5 cm^{-1}. Stable di-interstitials are formed when two self-interstitials are displaced in one damage event, and they are mobile at room temperature. In the initial stages of annealing the evolution of the point defects can be understood mainly in terms of trapping at the impurities. However, the positron signal shows that about two orders of magnitude more vacancies are produced by the protons than are detected in the point defects. Damage clusters exist, and are largely removed by annealing at 700 to 800 K, when there is an associated loss of broad band emission between 850 and 1000 meV. The well-known W center is generated by restructuring within clusters, with a range of activation energies of about 1.3 to 1.6 eV, reflecting the disordered nature of the clusters. Comparison of the formation of the X centers in oxygenated and oxygen-lean samples suggests that the J defect may be interstitial related rather than vacancy related. To a large extent, the damage and annealing behavior may be factorized into point defects (monitored by sharp-line optical spectra and DLTS) and cluster defects (monitored by positron annihilation and broadband luminescence). Taking this view to the limit, the generation rates for the point defects are as predicted by simply taking the damage generated by the Coulomb interaction of the protons and Si nuclei.

DOI: 10.1103/PhysRevB.73.165202 PACS number(s): 78.55.Ap, 61.72.Ji, 61.80.−x

I. INTRODUCTION

A major challenge to current semiconductor materials science is to understand the evolution of radiation damage caused by high-energy particles, as in ion implantation or irradiation with high-energy hadrons. In contrast, there is a massive literature on the radiation damage in silicon caused by small doses of low-energy (MeV) electrons. There, most of the radiation-induced effects are the result of the migration of vacancies and interstitial atoms to dopants. The structures of many of the defects are known, as outlined in Sec. V, and the evolution of the defects with annealing or increased dose can be modeled statistically.[1] The difficulties in understanding the radiation damage created by more energetic particles arise because they may displace more than one atom in each damage event. There are formidable problems in understanding these multiple displacements, such as the random configurations of the displaced atoms, how they interact to form stable groupings, how some of the clusters dissociate so that others may ripen and enlarge, the overlapping of different clusters of damage at high doses, and the dependence on the flux of the damaging ions. It is very difficult to make direct measurements on the clusters, but indirect techniques, such as modeling diffusion data, suggest that some clusters with four and eight self-interstitials are especially stable.[2] *Ab initio* modeling of even the simplest clusters is currently controversial. For example, clusters of three interstitials are predicted to be stable in different configurations[3–7] and have calculated migration energies of less than 0.23 eV (Ref. 3) or 1.7 eV.[6,7] Di-interstitials have been predicted to be very mobile at room temperature, with a migration energy of ~ 0.9 eV.[6,7] For the clusters of vacancies, a hexagonal ring of six vacancies is predicted to be stable,[8,9] and vacancy clusters are expected to be traps for hydrogen.[10] Very signifi-

cantly, vacancy clusters may also trap self-interstitials, opening up the possibility for rapid restructuring and stabilizing within a region of heavy damage.[11] A major problem in visualising the behavior of damage clusters is the large number of possible configurations of the defects, which may lead to unexpected stable structures.[5]

In this paper we will simplify the problem by considering the damage produced by very high-energy protons, of 24 GeV/c. From the Bethe-Bloch formula, a 24 GeV/c proton excites the electrons along its track in silicon at a mean rate of only ~84 meV per bond length.[12] Consequently, beam heating effects can be ignored, and the penetration length is many meters. The protons produce both simple Frenkel pairs and massive, localized damage. Underlying this paper is the recognition that the cross section for a 24 GeV/c proton to displace a Si atom is $\leqslant 1$ mb,[13] corresponding to the damage events being separated by several hundred Si atoms along the path of a proton. The radiation damage events are randomly distributed through a wafer, and they are nonoverlapping at the doses used here so that the damage is independent of the irradiation flux, in contrast to irradiation with protons of MeV energies.[14]

Because the individual damage events are sparse, they can be isolated from each other by carbon and oxygen atoms in the silicon, at least for annealing at less than 750 K. We will show that, to a good approximation, we may separate the damage into point-defect generation, which is monitored by sharp-line optical spectra and deep-level transient spectroscopy (DLTS), and cluster damage, which we show is monitored by positron annihilation and broadband luminescence. The rate at which the protons create simple point defects will be reported, Sec. III, and their evolution with annealing will be followed by observing the sharp-line luminesence features, Sec. V. Positron annihilation will be shown to measure predominantly the large clusters, Sec. IV, and will be correlated with a broad luminescence band, Sec. V B. Restructuring of some damage clusters is shown to result in production of the well-known W centers, Sec. V. Finally, we show that the quantitative data for the generation of the point defects can, surprisingly, be reproduced by simply considering the Coulomb interaction of the protons with the Si nuclei, Sec. VI. First, in Sec. II, we describe the experimental arrangements.

II. TECHNICAL DETAILS

The samples used for the infrared absorption measurements were 2 mm slices of Czochralski-grown silicon with high and low carbon content, one with $[O_i]=9\times10^{17}$ cm^{-3} and $[C_s]=7\times10^{16}$ cm^{-3}, and the other with $[O_i]=1.1\times10^{18}$ cm^{-3} and $[C_s]\sim10^{15}$ cm^{-3}. To generate sufficient absorption, they were irradiated with doses of 10^{16} cm^{-2} 24 GeV/c protons. The luminescence and positron annihilation studies were carried out on 300 μm wafers of float-zone silicon with 4 kΩ cm resistivity. The luminescence spectra showed evidence only for phosphorus as a shallow dopant, giving a concentration $[P]\sim10^{12}$ cm^{-3}. The carbon and oxygen contents were both close to the detection limits but were readily visible in the radiation effects, and so have concentrations of at least a few times 10^{15} cm^{-3}. Half the wafers have been used in their original state. The other half were diffused with oxygen to give a homogeneous concentration of $\sim10^{17}$ cm^{-3} by heating for 24 h at 1200 °C after growing a thermal oxide.[15,16] This type of material has been shown to increase the radiation tolerance of silicon radiation detectors[17] as a result of increasing the probability of vacancy-oxygen formation.[18,19] The samples for the luminescence and positron annihilation studies were irradiated to a nominal dose of 10^{14} cm^{-2}. A similar set of samples with phosphorus doping of 5×10^{12} was prepared for deep-level transient spectroscopy, with proton doses of $(1-2)\times10^{11}$ cm^{-2}. All the samples were irradiated at nominal room temperature using 24 GeV/c protons delivered in pulses of 400 ms length, each containing $(5-10)\times10^{10}$ protons cm^{-2}. The annealing stages used later were for 30 min at each temperature in an Ar atmosphere.

Absorption measurements were made using a Bruker 113v Fourier transform infrared spectrometer, in the range 400–4000 cm^{-1}, at a best spectral resolution of 0.5 cm^{-1}. Samples were cooled to 20 K using a closed circuit helium refrigerator for precise characterization of the spectra. To achieve the maximum signal-to-noise ratio for measurement of the strengths of the bands, spectra were remeasured at room temperature, at a cost of approximately halving the peak absorption as a result of line broadening.

The DLTS data were taken using a Semilab DLS-83D in the temperature range of 77 to 300 K by partial immersion in a liquid nitrogen bath. Heating and cooling scans were controlled to a rate of 0.2 K s during the 30 min required for each scan. The filling times used were 0.3 ms for minority carrier traps and 0.1 ms for majority carrier traps.

The photoluminescence data reported here were collected using a Bomem DA8 Fourier transform spectrometer fitted with a KBr beam splitter and a North-Coast fast-response Ge diode detector. The luminescence was excited with 514.5 nm Ar^+ laser light, with a power of 250 mW incident on the sample in a beam diameter of about 3 mm. It is absorbed with an exponential decay length of 1 μm. Since the samples are homogeneous with depth, the subsequent diffusion of excitons into the silicon[20] is unimportant. The spectra were collected with the samples mounted in a strain-free manner and either immersed in liquid helium at 4.2 K, or held in a helium drip-feed cryostat for variable-temperature measurements with a temperature stability of better than ~1 K for the range of 4.2 to 80 K. The relative intensities measured on different runs were standardized using the same reference sample and are estimated to be accurate to better than 25%, while line strengths change by orders of magnitude with annealing. The linewidth data were measured at a spectral resolution of 20 μeV. In this paper, the "width" of a zero-phonon line is the full width at half height, and "intensity" means that the emission has been integrated over the spectral extent of the line.

Positron annihilation was measured using an Ortec 583 fast-fast coincidence system with a time resolution of 245 ps. The ^{22}NaCl positron source was covered by a 1.5 μg cm^{-2}

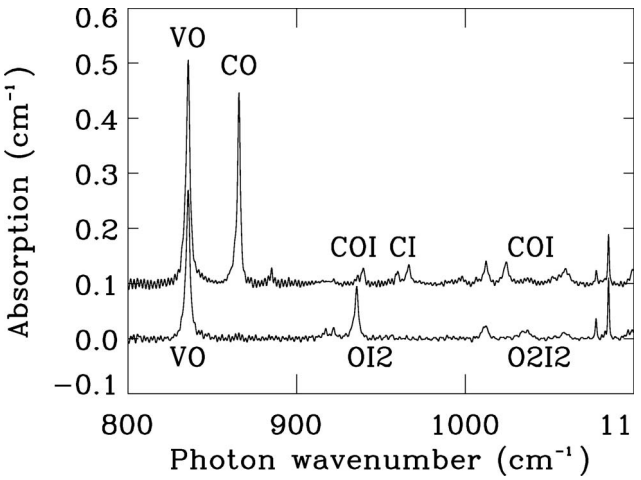

FIG. 1. Infrared absorption measured at 20 K in oxygen-rich samples with high carbon (upper curve, displaced by +0.1 cm^{-1} for clarity) and low carbon (lower curve). Radiation-induced peaks are labeled by their chemical origin, where for clarity the oxygen and carbon interstitials are simply labelled O and C. *I* is a self-interstitial, O2 the oxygen dimer, and 2*I* two self-interstitials. The 'CI' peak is a doublet. Other peaks are caused by oxygen interstitials and oxygen dimers.

Al foil and was sandwiched between two identical pieces of the samples. The mean penetration depth of the positrons is ~ 50 μm in silicon. A closed-cycle helium cryostat provided sample temperatures between 20 and 300 K, controlled to within ±1.5 K. Initially, the temperature-dependent positron trapping was observed in the temperature range of 20 to 300 K, (Fig. 2). Isochronal annealing was carried out by heating for 30 min in vacuum at each step of 50 K in the temperature range 300–1000 K, with the positron annihilation measured at 20 and 300 K.

III. MEASUREMENT OF THE POINT-DEFECT PRODUCTION RATE

Kuhnke *et al.*[21] have reported DLTS measurements which show a vacancy production rate of 1.0 ± 0.2 cm^{-1}, but an interstitial rate of 2.3–2.7 cm^{-1}. Their divacancy measurements were complicated by an overlapping unidentified feature, but was less than 1.4 cm^{-1}. We have remeasured the damage-production rates and extended the data as follows.

We first consider samples irradiated with 10^{16} cm^{-2} 24 GeV/*c* protons, to generate an accurately measurable infrared absorption (Fig. 1). With a high concentration of both oxygen and carbon, each single, mobile vacancy created by the protons will be captured by the oxygen, to generate an *A* center [a vacancy-oxygen (*V*-O), center). Using low-noise, room-temperature spectra and the known calibration constant for the 835 cm^{-1} A-center line,[22,23] the production rate of isolated vacancies is

$$\frac{d[V]}{dp} = 0.99 \pm 0.05 \text{ cm}^{-1}, \tag{1}$$

where the quoted uncertainty is limited to the precision of the present spectra, but the calibration factors themselves may be subject to an uncertainty of $\sim \pm 10\%$. In the same material, the self-interstitials are captured by carbon, creating interstitial carbon C_i, which mainly combines with oxygen to give *C*3, (C_i-O_i, centers. The damage is sufficient here to produce a small amount of *C*4 absorption (C_i-O_i-*I*, at 1024 cm^{-1} from a *C*3 center plus a self-interstitial. The calibration constants of *C*3 and *C*4 are known.[22] In addition, at room temperature, some C_i atoms survive for long enough to produce a small amount of C_i-*I* pairing, (Fig. 1). Since the calibration constants of *C*3 and *C*4 only differ by 15%, we *assume* that the constant for C_i-*I* is their mean. Remembering that the formation of each *C*4 center and each C_i-*I* requires two *I*'s, the rate of creation of isolated self-interstitials by the protons is

$$\frac{d[I]}{dp} = 1.0 \pm 0.05 \text{ cm}^{-1}, \tag{2}$$

where again the uncertainty is limited to that of the present spectra. A direct measurement of the loss of substitutional carbon following the irradiation can be made by using the 605 cm^{-1} line,[24] but it lies on intrinsic lattice absorption, giving considerable uncertainty in our measurement: the production of self-interstitials from the loss of carbon was estimated as $d[I]/dp = 1.35 \pm 0.25$ cm^{-1}.

The divacancy production rate has been derived by measuring the strength of the 2767 cm^{-1} band at low temperature, since the standard 1.8 μm band was unfortunately outside the range of the spectrometer used here. We have derived the calibration factor for the 2767 cm^{-1} band by using selected samples of oxygen-rich and carbon-rich silicon irradiated with 5 MeV neutrons or 10 MeV electrons, and measuring the production of the V_2O band at 833.5 cm^{-1} when the divacancies were annealed out at 550 K.[18] The calibration constant for the V_2O band was taken to be the same as for the 835 cm^{-1} line of *V*-O. The calibration factor for the divacancy obtained in our standard conditions (which may not be universally true) was $[V_2] = 5.5 \times 10^{15}$ αcm^{-3} for a peak 2767 cm^{-1} absorption of α (cm^{-1}). The divacancy production in the high-carbon samples used for Fig. 1 was

$$\frac{d[V_2]}{dp} = 0.47 \pm 0.05 \text{ cm}^{-1}, \tag{3}$$

with the uncertainty again being limited to the final spectrum.

In the sample with high oxygen and low carbon of Fig. 1 we identify a peak at 936 cm^{-1} with a di-interstitial-oxygen complex,[25] which is not observed in electron-irradiated samples. Assuming (for want of a better factor) that the calibration constant is the same as for *V*-O, the introduction rate of I_2 is

$$\frac{d[I_2]}{dp} \sim 0.3 \text{ cm}^{-1}, \tag{4}$$

which is similar to the value for V_2, Eq. (3). Equations (3) and (4) suggest that when two vacancies and interstitials are created simultaneously in a small cluster, they form a stable divacancy *and* a stable, mobile I_2, as has been predicted by *ab initio* theory.[6,7]

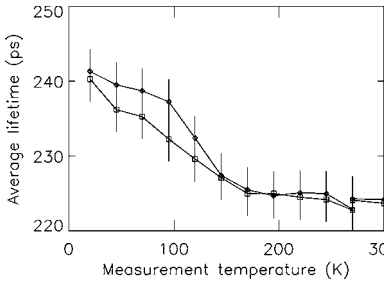

FIG. 2. The average lifetimes of the positrons as functions of the measurement temperature in the oxygenated (diamonds) and nonoxygenated (squares) samples, in the as-irradiated state.

As further confirmation of the introduction rates, we have irradiated samples with 10^{11} cm^{-2} 24 GeV/c protons, so that the DLTS signals of the 0.17 eV electron trap of the A center and the 0.36 eV hole trap of the C_i-O_i center were measurable. The creation rate of the A center was 1.0 ± 0.15 cm^{-1}, and that of the C_i-O_i center was 1.1 ± 0.15 cm^{-1}, again confirming Eqs. (1) and (2). From the DLTS measurements, the production rate of the V_2^{2-} was $\sim$0.2 cm^{-1}, and that of V_2^- plus a superimposed unknown species was 1.0 ± 0.2 cm^{-1}, at least not inconsistent with Eq. (3).

IV. POSITRON ANNIHILATION

A strong defect-related positron annihilation signal can be obtained from samples irradiated with 10^{14} cm^{-2} protons. Figure 2 shows the average lifetimes of the positrons as functions of the measurement temperature in the oxygenated and the nonoxygenated samples, in the as-irradiated state. Measurement sensitivity is best at the lowest temperatures, partly because the thermal release of trapped positrons is minimised, and partly because the diffusion of the excitons is reduced at higher temperatures by scattering from acoustic phonons.[26] The positron lifetime, measured at 20 K, behaves in very similar ways in the oxygenated and the oxygen-free materials, with an almost constant lifetime to an annealing temperature of 700 K, and then a decrease between 700 and 900 K to the level of the un-irradiated reference sample (Fig. 3). The vacancy aggregates reduce severely in concentration at these temperatures, as observed for silicon irradiated with low-energy protons.[27]

The lifetime τ of a positron trapped at a vacancy defect is increased from its value of $\tau_{\text{bulk}}=218$ ps in perfect bulk silicon[28] as a result of the decreased electron density.[29] For trapping at neutral monovacancies, $\tau_v=270-275$ ps.[28] As the number of vacancies n in a cluster increases, τ increases, but only slowly with n. The lifetimes calculated by Staab *et al.*[9] for the *most compact* clusters containing n vacancies can be fitted approximately by $\tau(n)=220+230[1-\exp(-n/5)]$ ps, a range of only a factor of 2. The lifetime is predicted to be independent of n for positrons trapped at hypothetical *linear* vacancy chains,[9] and divacancies and a tetravacancy are predicted to have very similar positron lifetimes.[11] The slow variation is confirmed by experimental studies of silicon damaged by low-energy protons: the optical signal specific to divacancies disappears at one annealing stage as the vacancies restructure, while the positron signal remains unchanged.[27] The defect-related lifetime found here, $\sim$300 ps, suggests small clusters, say with $n<6$ vacancies. The clusters, with an unknown distribution of sizes and forms, are represented here by an "equivalent defect." The trapping rate K at the equivalent defects is given by the average lifetimes τ_{av}, τ_{bulk}, and τ_{def} by[26]

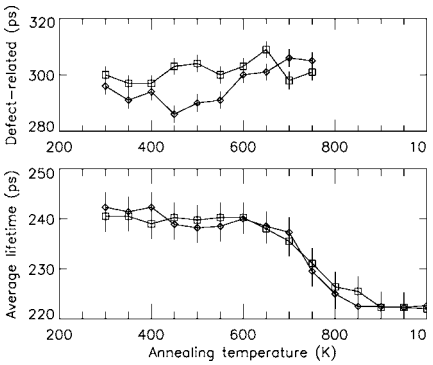

FIG. 3. Lower figure shows the average lifetime of the positrons, measured at 20 K, in the oxygenated (diamonds) and nonoxygenated (squares) samples, following annealing at 50 K stages. The upper plot shows the defect-related lifetimes derived from the measured data.

$$K=\frac{1}{\tau_{\text{bulk}}}\frac{\tau_{\text{av}}-\tau_{\text{bulk}}}{\tau_{\text{def}}-\tau_{\text{av}}}. \tag{5}$$

The trapping rate is related to the concentration c of traps and the trapping coefficient μ by $K=\mu c$. For $n<6$, we assume that μ is proportional to the number n of vacancies in each trap,[30] $\mu=n\mu_1$ where μ_1 is the trapping coefficient μ_1 for a monovacancy. Then, the total concentration C_v of vacancies in the traps is independent of the size of the equivalent defect, $C_v=nc=K/\mu_1$. The trapping coefficient for monovacancies is only known at room temperature, when[31] $\mu_1\sim1\times10^{15}$ s^{-1}. Evaluating with $\tau_{\text{av}}=223$ ps, Fig. 2, $\tau_{\text{bulk}}=216$ ps, and $\tau_{\text{def}}\sim300$ ps, Fig. 3, gives a fractional concentration

$$C_v\sim3\times10^{-7}\equiv1.5\times10^{16}\ \text{cm}^{-3}, \tag{6}$$

for the nonoxygenated material and $\sim$7% larger for the oxygenated. We anticipate that C_v is correct within a factor of about 2. The rate of creating the vacancies in clusters is

$$\frac{d[V_c]}{dp}\sim1.5\times10^2\ \text{cm}^{-1}. \tag{7}$$

The production rate detected by positrons is two orders of magnitude greater than the point-defect values, Eqs. (1)–(4).

V. LUMINESCENCE DATA

Before irradiation (Fig. 4), the luminescence spectra show only emission from the phosphorus donors and pure silicon plus, in the oxygenated samples, weak emission from the 808

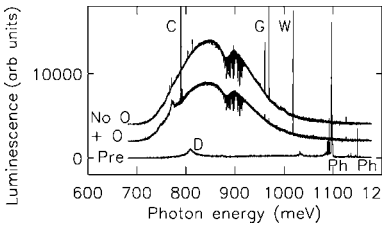

FIG. 4. Preirradiation, both materials show identical luminescence above 1000 meV from the phosphorus donors ("Ph") plus weak free-exciton emission. The oxygenated material, labeled "Pre," also contains weak dislocation bands at 808 and 874 meV. After irradiation, the high-energy luminescence is quenched, and both materials show a broadband between about 750 and 1000 meV, plus weak *W* emission at 1018 meV. In the oxygenated sample ("+O"), carbon interstitials have been trapped preferentially at oxygen, forming the C center (789 meV), and in the non-oxygenated sample ("No O") preferentially at substitutional carbon, creating the *G* center (969 meV). The sharp absorption lines and the dip near 800 meV are from atmospheric and instrumental absorption. The spectra shown here were measured at 4.2 K and at 60 μeV resolution.

and 875 meV D_1 and D_2' dislocation features. Irradiation with 10^{14} cm^{-2} protons destroys the emission from the phosphorus (Fig. 4). Since the concentration of the phosphorus atoms, [P]$\sim 10^{12}$ cm^{-3}, is much lower than the background level of oxygen, the phosphorus is unlikely to capture vacancies, and the removal of the luminescence originating at the phosphorus is a result of charge transfer to the radiation defects. However, the damage centers have concentrations orders of magnitude larger than [P], Secs. III and IV, and so we can ignore the effect on the damage centers of transfering the charge.

A. Sharp-line luminescence spectra

We recall that a mobile monovacancy (V) will be trapped at an O_i atom, giving an A center, which is stable to $\sim$600 K.[18] The A center then moves to give $VO+O \rightarrow VV_2$ which is stable to 750 K. The great majority of the V's are stored in these VO_i and VO_2 centers to 750 K. Then, with some loss of V's elsewhere, VO_3 is produced through the motion of a highly mobile form of VO_2.[32] All these centers are nonluminescent.

Single self-interstitials created by the protons react with a substitutional carbon atom C_s to create a carbon interstitial C_i, which will combine with a second C_s atom to generate a G center, or C_i will react with oxygen O_i to generate a C center.[24] The branching ratio is proportional to the ratio of the concentrations of C_s and O_i.[22] Consequently, the C line (at 789.5 meV) is the dominant sharp-line emission after irradiation in the oxygenated material, and the dicarbon G center (969.5 meV) is dominant when the carbon content is comparable to or greater than the oxygen content (Fig. 4).

Annealing at 300 to 425 K shows an increase by up to a factor of 2 in the thermally stable C luminescence band (C_i -O_i) band (Fig. 5). The width of the C line increases marginally during this annealing stage (Fig. 6), consistent with the creation of new C centers close to the strain field of damage clusters. The conclusion is that in the range 300–425 K, self-interstitials may be liberated from clusters, but only in concentrations up to the original creation rate of single interstitials, Eq. (2).

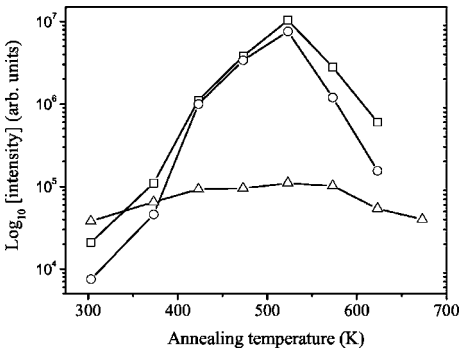

FIG. 5. Intensities of the *W* and *C* zero-phonon lines, measured at 4.2 K. Squares and circles are for the *W* line in non-oxygenated and oxygenated samples, respectively. The triangles are for the *C* line in the oxygenated samples. The relative uncertainties in the intensities are comparable to the heights of the symbols.

Annealing at 525 K results in the destruction of the G band and the carbon sequence continues with the formation of the T center (935.1 meV, a dicarbon-hydrogen center[33]). In oxygen-rich material, the C line is destroyed above 600 K, and the P line at 767 meV grows; the P center is very similar to the C center, and possibly is a C center perturbed by a second oxygen atom.[34] P is stable to $\sim$775 K, and its range of stability overlaps with that of the H center (925.6 meV, a carbon-oxygen center[35]) which is created at $\sim$700 K and destroyed at 825 K. This is the limit of stability of the known carbon-oxygen damage centers.

In both oxygen-rich and -lean material, a line at 760.9 meV is detected at 725 K and is destroyed by 925 K. The energy coincides with the energy of the M line, which occurs at a monoclinic I, carbon plus hydrogen center,[36] although the M line has previously been reported to be stable only to 625 K.[37] Its intensity is a few times larger in the

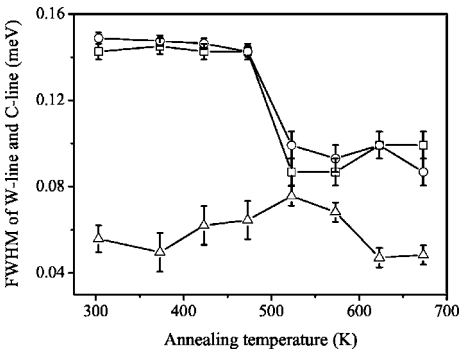

FIG. 6. Full widths at half height of the *W* and *C* zero-phonon lines, measured at 4.2 K. Squares and circles are for the *W* line in nonoxygenated and oxygenated samples, respectively. The triangles are for the *C* line in the oxygenated samples. The data were obtained at a spectral resolution of 20 μeV.

nonoxygenated material, which would be consistent with the center occuring at a carbon-related, oxygen-free center like *M*. The 760.9 meV line is accompanied by two weaker lines at 761.2 and 761.3 meV, which occur at independent centers, and which could be uniquely perturbed versions of the 760.9 meV center. The *T* line (935.1 meV) also has two weaker satellites, 0.6 and 0.8 meV, to higher energy (cf. 0.4 and 0.5 meV for the *M* line's satellites).

In addition to the carbon lines, the *W* line (1018 meV) appears immediately after irradiation. This defect is not generated by low doses of electron damage,[38] but requires bombardment capable of producing clusters. It has trigonal symmetry,[39] and has no dependence on impurities. Models proposed include a monointerstitial[38] and a di-interstitial,[38,40] but both of these are highly mobile (Secs. I and III). The center may be constructed from three silicon interstitial atoms,[3] but the compact structure has been predicted to not produce the observed local vibrational modes,[41] and the configuration of 3 self-interstitials is uncertain (Sec. I). The *W* center has similar creation and destruction conditions to those of the paramagnetic *B*5 center, but there is no confirmed model for that center.[42] Since the location of the *W* centers is beyond the range of ions in implanted Si,[40] we will assume that they are small self-interstitial clusters.

The *W* line grows considerably in strength on annealing from room temperature to 525 K (Fig. 5). The intensity and width of the *W* line have exactly the same characteristics in both oxygenated and oxygen-lean material (Figs. 5 and 6), as expected for events that occur *within* the clusters, and so are independent of the impurity in the bulk of the crystal. The width data confirm that the *W* centers are being created in the damage-cluster regions. Before annealing, and through its growth phase, the *W* line is almost three times wider than the *C* line (Fig. 6), even though, from their responses to strains,[39,43] equal random strain fields would make the *W* line 35 times *sharper* than the *C* line: the *W* centers are severely strained compared to the *C* centers which lie in the bulk crystal. The increased *W* luminescence could be the result of a dramatic increase in luminescence efficiency of existing *W* centers, since vacancy clusters are known to be strong nonradiative traps in ion-implanted silicon.[44] However, there is no significant change in the positron signal at these temperatures, and we will show in Sec. V B that the broad luminescence features associated with the damage clusters only increase in intensity by a small factor. The increase in *W* emission is therefore because the concentration of centers has increased, at clusters. The formation of the *W* centers involves motion of interstitial atoms by only a small number *N* of steps, and takes approximately $\tau=30$ min at $T=425-525$ K. The effective formation barrier is $E\sim kT\ln(\nu_0\tau/N)$, giving $E\sim 1300-1600$ meV for an attempt frequency $\nu_0=10^{13}$ Hz and assuming $N=5$ sequential steps. A range of effective formation energies would be expected, given the disordered cluster damage.

Evidence that a further structural change in the clusters, reducing their strain, occurs at 525 K comes from the sudden decrease in width of the *W* line (Fig. 6), while the *W* line is still growing in intensity.

Above 525 K, the *W* centers are destroyed (Fig. 5). The annealing temperature would suggest an activation energy of

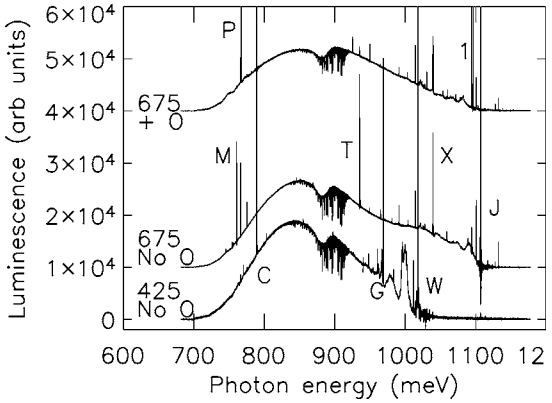

FIG. 7. After 425 K annealing, both materials are developing strong, and identical, *W* bands. The nonoxygenated sample shown here, bottom spectrum, has the *G* (969 meV) and *C* (789 meV) lines; the oxygenated has a negligible *G* line and the *C* line is 4.5 times stronger. By 675 K, the strongest features are the *J* lines in the nonoxygenated (second spectrum from bottom), and the 1096 meV line, labeled 1, and the *P* line in the oxygenated material (top spectrum). The sharp absorption lines and the dip near 800 meV are from atmospheric and instrumental absorption. The spectra shown here were measured at 4.2 K and at 60 μeV resolution.

only $E_m\leqslant 2$ eV for a long-range migration process, little more than the formation energy of the *W* center estimated above. There is still no appreciable change in the positron signal to suggest vacancy-interstitial recombination, but E_m is close to the value predicted for the mobility of some I_3 clusters.[6,7]

A difference in behaviour of the oxygen-doped and oxygen-lean samples occurs as the *W* centers are destroyed above 525 K. In the oxygen-doped samples, a luminescence band at 1096.9 meV is produced, (Figs. 7 and 8), as in neutron-irradiated Czochralski samples.[45] The 1096.9 meV center is a monoclinic *I* center that contains oxygen.[45] Since it is produced at temperatures at which the oxygen is immobile and the *V*-O center is still stable, the center may be the result of self-interstitials being captured by oxygen.[45] At this stage, the self-interstitials that were mobile in the crystal at lower temperatures are still locked in the carbon-oxygen *C* centers (Fig. 5). The source of the *I*'s may be the *W* centers. The 1096.9 meV line diminishes above 675 K, is briefly replaced by a line at 1101.2 meV (Fig. 9) that does not occur in the oxygen-free samples, and the *X* defect, zero-phonon line at 1039.5 meV, then becomes a dominant feature of the spectra. The *X* defect has been suggested to be a tetrainterstitial.[46] That suggestion is consistent with the isotope-induced behavior of its local vibrational modes,[47] and with its recent identification with the *B*3 paramagnetic center, ascribed to a tetrainterstitial.[42]

In contrast, in the oxygen-lean material, the 1096.9 meV system is not created, but instead the *J* system appears (1106.8 and 1107.6 meV). There is no change in the positron signal to suggest modifications to the vacancies. The *J* center has been ascribed to a hexavacancy plus hydrogen complex.[10] However, as the *J* system anneals out, the *X* line and the 991 meV line appear, as though the *J* system is play-

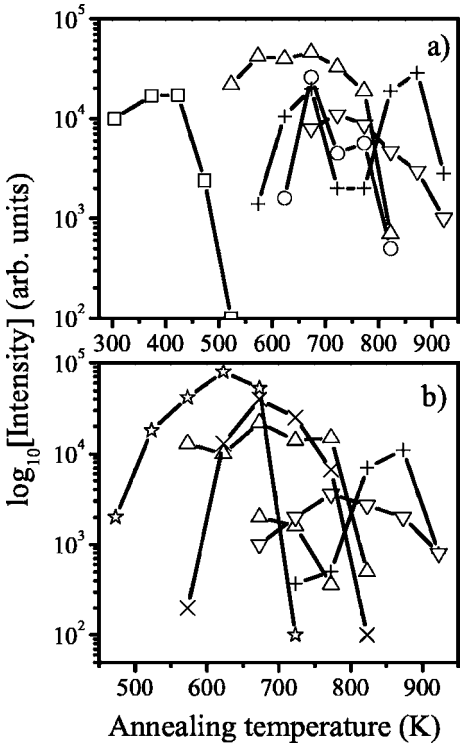

FIG. 8. Intensities of the luminescence from zero-phonon lines as functions of annealing in the nonoxygenated samples (a) and the oxygenated samples (b). Data are shown by squares for the G line, circles for the T line, triangles for the X line, + for the M line, inverted triangles for the 991 meV line, × for the P line, and ⋆ for the 1096 meV line. The relative uncertainties in the intensities are comparable to the heights of the symbols.

ing an analogous role in oxygen-free material to that of the 1096.9 meV line in oxygen-doped material. The 991 meV line occurs at a trigonal center of unknown chemical composition,[48] and is observed between 725 and 925 K (Fig. 9). The line has similar strengths in the oxygen-free and oxygenated materials at the same stages of annealing, implying that the center does not contain oxygen.

B. The broad spectral features

Although luminescence from the sharp-line features are easy to observe, most of the total emission in the spectra comes from the broad background underlying the sharp-line structure. Broad bands are often observed after irradiation by particles that create heavy damage, or after large doses of electron irradiation, and it is likely to come from disordered regions of unknown stucture in the silicon. The broadbands have the same shapes in the oxygenated and nonoxygenated samples, implying that there is negligible decoration by oxygen of the damage clusters.

The intensity of the broad emission, integrated over from 680 to 930 meV, where it is free of strong vibronic bands, is shown in Fig. 10. In both types of material, the intensity increases by a small factor up to ~550 K. This is the range where the W line is increasing, which was shown in Sec. V A to be caused by restructuring within small clusters. The increase in broadband emission may simply be a result of increasing luminescence efficiency as the heavily damaged regions restructure, but on the scale of most of the other intensity changes, the increase is small. Between 525 and 675 K the broad emission from the oxygenated material is quenched by a factor of 3, in contrast to the nonoxygenated (Fig. 10), with no apparent change in spectral shape. However, for both materials, annealing above 675 K produces a sudden decrease in the intensity of the higher-energy part of the broad emission (Fig. 9) at the same temperatures as the positron signal from the defects becomes negligible (Fig. 3). The loss implies that the broad emission centered on 930 meV is caused by vacancies. The low en-

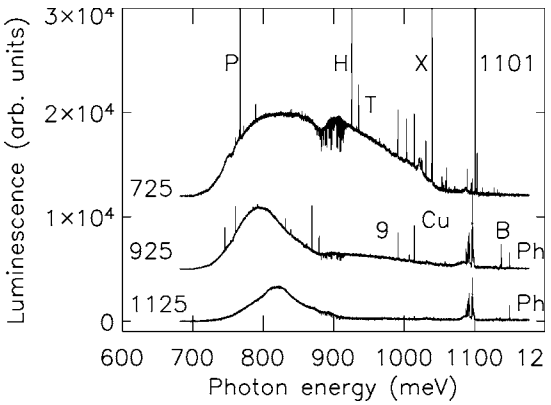

FIG. 9. Spectra are for the oxygenated material; very similar spectra are observed in the nonoxygenated material, with the intensities of the M, P, H, and T lines depending on the carbon and oxygen content (Sec. V). By 725 K, top spectrum, the X (1049 meV) and 991 meV 9 lines are present equally in both materials, but the 1101.2 meV line 1101 only occurs in the oxygenated material. At 925 K the broad background luminescence has been reduced mainly to a sharper peak, apparently centered on 800 meV, but distorted by the low-energy cutoff of the spectrometer system. New lines are seen at 1138 meV from the B_{71}^{1} system, labeled B. The phosphorus "Ph" emission is again detectable, and other point-defect features are reducing, to disappear by 1125 K (bottom spectrum). The line "Cu" at 1014 meV is from copper contamination introduced during the heat treatment. The sharp absorption lines and the dip near 800 meV are from atmospheric and instrumental absorption. The spectra shown here were measured at 4.2 K and at 60 μeV resolution.

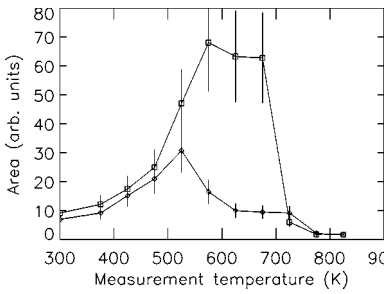

FIG. 10. Variation of the intensity of the broad background band measured at 4.2 K, integrated from 680 to 930 meV, in the oxygenated (diamonds) and nonoxygenated (squares) samples, following annealing in 50 K stages.

ergy emission remains to the highest annealing temperatures 1125 K (Fig. 9), when the positron signal is indistinguishable from that of the virgin sample. At 925 K the signal from phosphorus begins to recover, presumably as the general damage level reduces so that the donors are no longer ionized.

VI. COULOMB SCATTERING OF 24 GeV/*c* PROTONS

Huhtinen has presented a comprehensive description of the damage process when silicon is irradiated with 24 GeV/*c* protons.[13] Given our present limited knowledge (Sec. I), the model necessarily required many assumptions, and it led to predicting the creation rate of divacancies to equal that of monovacancies, in contrast to observation (Sec. III). In this paper, we have found that the damage may be divided into point defect and cluster damage. A simplistic picture is to assume that the cluster damage comes from nuclear interactions of a proton and a nucleus, and that point defects come from the long range Coulomb interaction. The Coulomb interaction is by far the simpler, and the statistics of its damage are now briefly considered.

The proton travels within 0.1% of the speed c of light, and transfers, by the Coulomb interaction, an energy $E=(Ze^2/2\pi\epsilon_0 c)^2(1/2Mr^2)$ to a Si nucleus of mass M, giving $E=k/r^2$ where $k=3.1\times10^{-26}$ when E is in eV and the impact parameter (nearest approach distance) r is in meters. To displace a Si atom requires $E>15$ eV,[49] requiring $r<4.5\times10^{-14}$ m. The probability of transfering an energy E to $E+dE$ to a nucleus is $P(E)dE=k/(R^2E^2)dE$, where, from the atomic density of Si, the normalization radius $R=0.153$ nm. The probability of transfering more than $E_d=15$ eV to a nucleus that it passes is then 3×10^{-8} (changing only to 2×10^{-8} if $E_d=25$ eV). For the proton dose of 10^{14} cm^{-2} used in Secs. IV and V, the damage events are separated on average by $s\approx800$ atoms, twice as big as the mean separation of impurities at a background defect concentration of 10^{15} cm^{-3}, and ten times larger than for the oxygen atoms at 10^{17} cm^{-3}.

Further displacements of Si nuclei by the primary knock-on atom (PKA) have been calculated by TRIM.[49] The mean number of atoms displaced by a PKA of energy E is fitted by $\bar{n}=a(E-20)^q$, where $a=0.059$, $q=0.9$, for $E<2\times10^4$ eV. The actual number n of vacancies created by the PKA may be $0,1,2\ldots(E-E_d)/E_d$. The probability $p(n)$ that a PKA of energy E creates a further n vacancies is found to be given closely by a Poisson distribution, $p(n)=\bar{n}^n\exp(-\bar{n})/n!$. Knowing the energy distribution of the PKAs, and the Poisson statistics for producing further knock-out atoms, we may predict the distribution of the damage events that produce different numbers of vacancies (Fig. 11). The rates of creation (per proton) of single vacancies V and single self-interstitials I, and of simultaneously producing two vacancies V_2 and two self-interstitials I_2 are predicted to be

$$\frac{d[V]}{dp}=\frac{d[I]}{dp}=1.0\ \text{cm}^{-1},\quad \frac{d[V_2]}{dp}=\frac{d[I_2]}{dp}=0.51\ \text{cm}^{-1}. \tag{8}$$

These values are surprisingly similar to the measured values, Eqs. (1)–(4). However, we emphasize that we have ignored the destruction of a high fraction of the point defects through correlated vacancy-interstitial recombination, and also the creation of point defects in the more massive impacts.

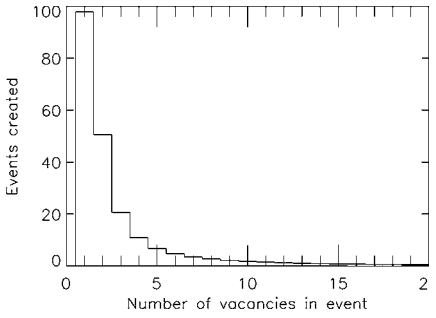

FIG. 11. Calculations, using the simple model of Sec. VI for the damage created in a cube of side 1 μm by irradiation with 10^{14} cm^{-2} protons, of the number of damage events which generate different total numbers of vacancies. There are about 100 damage events creating monovacancies, about 50 creating a total of two vacancies, and so on. The maximum energy of the PKA considered is 1500 eV, when the probability of occurence is only 0.01% of the probability of a nucleus being displaced with 15 eV.

VII. SUMMARY

We have reported on the irradiation of silicon, at room temperature, by fast protons. We have chosen irradiation doses and suitable concentrations of carbon and oxygen, so that the mobility of damage products may be followed. We have reported the creation rates of single vacancies, single self-interstitials, divacancies, and diinterstitials (Sec. III). Stable, mobile, di-interstitials are created at very similar rates to divacancies (Sec. III). However, the total production of damage is two orders of magnitude larger than is accounted for by the point defects, and takes the form of small clusters (Sec. IV). These clusters, formed at room temperature, are initially stable to annealing: some interstitial emission (but only ~1% of the total interstitials) is detected on annealing at 300 to 425 K, and there is evidence for restructuring within clusters at 300 to 525 K (Sec. V A). The vacancy clusters are removed by annealing at 700 to 800 K, (Sec. IV), when there is an associated loss of broadband luminescence (Sec. V B).

Because the point defects are generated in each pulse of protons (Sec. II) at a rate three orders of magnitude smaller than was modeled for electron damage,[22] the evolution with annealing of the point defects closely follows the pattern established for electron damage (Sec. V), with mobile defects moving to impurities. This picture contradicts the model that the C_i-related defects are generated in the clusters, a model suggested by the charge-filling statistics of those centers as observed in DLTS from material that was very similar to our oxygen-free samples.[21]

To a surprising extent, it appears to be possible to separate the damage into point defects and cluster defects, certainly for annealing below 575 K. With the techniques used here,

point defects are monitored by sharp-line optical spectra and DLTS, and vacancy clusters by positron annihilation and broadband luminescence. Taking this view to the limit, the generation rates for the 'point defects' turn out to be, surprisingly, as predicted by simply taking the immediate damage generated by the Coulomb interaction of the proton and Si nuclei (Sec. VI).

ACKNOWLEDGMENTS

We thank Michael Moll and the CERN RD-50 collaboration for use of the irradiation facility at CERN. L.M. thanks the Royal Society and A.S. thanks Deutscher Akademischer Ausstauschdienst and the Martin-Luther University-Halle-Wittenberg, for support.

*Electronic address: gordon.davies@kcl.ac.uk

[1] B. MacEvoy and G. Hall, Mater. Sci. Semicond. Process. **3**, 243 (2000).
[2] N. E. B. Cowern, G. Mannino, P. A. Stolk, F. Roozeboom, H. G. A. Huizing, J. G. M. van Berkum, F. Cristiano, A. Claverie, and M. Jaraiz, Phys. Rev. Lett. **82**, 4460 (1999).
[3] S. K. Estreicher, M. Gharaibeh, P. Fedders, and P. Ordejon, Phys. Rev. Lett. **86**, 1247 (2001).
[4] B. J. Coomer, J. P. Goss, R. Jones, S. Oberg, and P. R. Briddon, Physica B **273-274**, 505 (1999).
[5] D. A. Richie, J. Kim, S. A. Barr, K. R. A. Hazzard, R. Hennig, and J. W. Wilkins, Phys. Rev. Lett. **92**, 045501 (2004).
[6] M. Cogoni, B. P. Uberuaga, A. F. Voter, and L. Colombo, Phys. Rev. B **71**, 121203(R) (2005).
[7] M. Posselt, F. Gao, and D. Zwicker, Phys. Rev. B **71**, 245202 (2005).
[8] S. K. Estreicher, J. L. Hastings, and P. A. Fedders, Appl. Phys. Lett. **70**, 432 (1997).
[9] T. E. M. Staab, M. Haugk, A. Sieck, T. Frauenheim, and H. S. Leipner, Physica B **273-274**, 501 (1999).
[10] B. Hourahine, R. Jones, A. N. Safonov, S. Oberg, P. R. Briddon, and S. K. Estreicher, Phys. Rev. B **61**, 12594 (2000).
[11] D. V. Makhov and L. J. Lewis, Phys. Rev. Lett. **92**, 255504 (2004).
[12] J. F. Ziegler, J. Appl. Phys. **85**, 1249 (1999).
[13] M. Huhtinen, Nucl. Instrum. Methods Phys. Res. A **491**, 194 (2002).
[14] P. Leveque, A. Hallen, P. Pellegrino, B. G. Svensson, and V. Privitera, Nucl. Instrum. Methods Phys. Res. B **186**, 375 (2002).
[15] G. Lindstroem and R. D. 48-Collaboration, Nucl. Instrum. Methods Phys. Res. A **466**, 308 (2001).
[16] L. Fonseca, M. Lozano, F. Campabadal, C. Martinez, M. Ullan, B. S. Avset, A. Ruzin, F. Lemeilleur, and E. Nossarzewska-Orlowska, Microelectron. Reliab. **40**, 791 (2000).
[17] M. Bruzzi and R. D. 50-Collaboration, Nucl. Instrum. Methods Phys. Res. A **541**, 189 (2005).
[18] J. L. Lindstroem, L. I. Murin, T. Hallberg, V. P. Markevich, B. G. Svensson, M. Kleverman, and J. Hermansson, Nucl. Instrum. Methods Phys. Res. B **186**, 121 (2002).
[19] I. Pintilie, E. Fretwurst, and G. Lindstrom, Appl. Phys. Lett. **82**, 2169 (2003).
[20] M. Nakamura, T. Suzuki, and M. Fujita, Phys. Rev. B **35**, 2854 (1987).
[21] M. Kuhnke, E. Fretwurst, and G. Lindstroem, Nucl. Instrum. Methods Phys. Res. A **485**, 140 (2002).
[22] G. Davies, E. C. Lightowlers, R. C. Newman, and A. S. Oates, Semicond. Sci. Technol. **2**, 524 (1987).
[23] A. S. Oates, R. C. Newman, J. M. Tucker, G. Davies, and E. C. Lightowlers, in *Oxygen, Carbon, Hydrogen, and Nitrogen in Crystalline Silicon*, edited by J. C. Mikkelsen, S. J. Pearton, J. W. Corbett, and S. J. Pennycook MRS Symposia proceedings No. 59 (Materials Research Society, Pittsburgh, 1986), p. 59.
[24] G. Davies and R. C. Newman, in *Handbook on Semiconductors*, edited by T. S. Moss and S. Mahajan (Elsevier, Amsterdam, 1994), Vol. 3, p. 1557.
[25] J. Hermansson, L. I. Murin, T. Hallberg, V. P. Markevich, J. L. Lindstroem, M. Kleverman, and B. G. Svensson, Physica B **302-303**, 188 (2001).
[26] J. Gebauer, F. Rudolf, A. Polity, R. Krause-Rehburg, J. Martin, and P. Becker, Appl. Phys. A: Mater. Sci. Process. **68**, 411 (1999).
[27] R. Poirier, V. Avalos, S. Dannefaer, F. Schiettekatte, and S. Roorda, Nucl. Instrum. Methods Phys. Res. B **206**, 85 (2003).
[28] S. Dannefaer, Phys. Status Solidi A **102**, 481 (1987).
[29] R. Krause-Rehberg and H. S. Leipner, *Positron Annihilation in Semiconductors* (Springer, Berlin, 1999).
[30] R. M. Nieminen and J. Laakonen, Appl. Phys. **20**, 181 (1979).
[31] R. Krause-Rehberg, A. Polity, and T. Abgarjan, Mater. Sci. Forum **175-178**, 427 (1995).
[32] J. L. Lindstroem, L. I. Murin, B. G. Svensson, V. P. Markevich, and T. Hallberg, Physica B **340-342**, 509 (2003).
[33] A. N. Safonov, E. C. Lightowlers, G. Davies, P. Leary, R. Jones, and S. Oberg, Phys. Rev. Lett. **77**, 4812 (1996).
[34] W. Kurner, R. Sauer, A. Dornen, and K. Thonke, Phys. Rev. B **39**, 13327 (1989).
[35] E. C. Lightowlers and A. N. Safonov, Mater. Sci. Forum **258-262**, 617 (1997).
[36] A. N. Safonov, E. C. Lightowlers, and G. Davies, in *Proceedings of the International Conference on Semiconductors*, edited by D. J. Lockwood (World Scientific, Vancouver, 1994), Vol. 3, p. 2239.
[37] E. Irion, N. Burger, K. Thonke, and R. Sauer, J. Phys. C **18**, 5069 (1985).
[38] M. Nakamura and S. Nagai, Phys. Rev. B **66**, 155204 (2002).
[39] G. Davies, E. C. Lightowlers, and Z. E. Ciechanowska, J. Phys. C **20**, 191 (1987).
[40] P. K. Giri, Semicond. Sci. Technol. **20**, 638 (2005).
[41] G. M. Lopez and V. Fiorentini, J. Phys.: Condens. Matter **15**, 7851 (2003).
[42] D. Pierreux and A. Stetsmans, Phys. Rev. B **71**, 115204 (2005).
[43] C. P. Foy, M. C. do Carmo, G. Davies, and E. C. Lightowlers, J. Phys. C **14**, L7 (1981).
[44] R. Harding (private communication).
[45] F. Rodriguez, G. Davies, and E. C. Lightowlers, Radiat. Eff. Defects Solids **149**, 141 (1999).
[46] R. Jones, T. A. G. Eberlein, N. Pinho, B. J. Coomer, J. P. Goss, P.

R. Briddon, and S. Oberg, Nucl. Instrum. Methods Phys. Res. B **186**, 10 (2002).
[47] S. Hayama, G. Davies, and K. M. Itoh, J. Appl. Phys. **96**, 1754 (2004).
[48] J. Gower, E. C. Lightowlers, G. Davies, and A. N. Safonov, in *Early Stages of Oxygen Precipitation in Silicon*, edited by R. Jones (Kluwer Academic Publishers, Amsterdam, 1996), p. 463.
[49] J. Ziegler, www.srim.org.